ISSN 1063-7788, Physics of Atomic Nuclei, 2013, Vol. 76, No. 10, pp. 1213–1218. © Pleiades Publishing, Ltd., 2013.
Original Russian Text © V.V. Ammosov, N.N. Antonov, A.A. Baldin, V.A. Viktorov, V.A. Gapienko, G.S. Gapienko, A.A. Golovin, V.N. Gres, A.A. Ivanilov, V.I. Koreshev, V.A. Korotkov, A.I. Mysnik, A.F. Prudkoglyad, Yu.M. Sviridov, A.A. Semak, V.I. Terekhov, V.Ya. Uglekov, M.N. Ukhanov, B.V. Chujko, S.S. Shimanskii, 2013, published in Yadernaya Fizika, 2013, Vol. 76, No. 10, pp. 1275–1280.

ELEMENTARY PARTICLES AND FIELDS
Experiment

Measurement of the Yields of Positively Charged Particles at an Angle of 35° in Proton Interactions with Nuclear Targets at an Energy of 50 GeV

V. V. Ammosov[†1)], N. N. Antonov[1)], A. A. Baldin[2)], V. A. Viktorov[1)], V. A. Gapienko[1)], G. S. Gapienko[1)], A. A. Golovin[1)], V. N. Gres[1)], A. A. Ivanilov[1)], V. I. Koreshev[1)], V. A. Korotkov[1)], A. I. Mysnik[1)], A. F. Prudkoglyad[1)], Yu. M. Sviridov[1)], A. A. Semak[1)*], V. I. Terekhov[1)], V. Ya. Uglekov[1)], M. N. Ukhanov[1)], B. V. Chujko[1)], and S. S. Shimanskii[2)]

Received May 3, 2012

Abstract—Momentum spectra of cumulative particles in the region of high transverse momenta (P_T) in $pA \to h^+ + X$ reactions were obtained for the first time. The experiment in which this was done was performed at the SPIN setup (Institute for High Energy Physics, Protvino) in a beam of 50-GeV protons interacting with C, Al, Cu, and W nuclei. Positively charged particles were detected at a laboratory angle of 35° and in the transverse-momentum range between 0.6 and 3.7 GeV/c. A strong dependence of the particle-production cross section on the atomic number was observed. A comparison with the results of calculations based on the HIJING and UrQMD models was performed in the subcumulative region.

DOI: 10.1134/S1063778813100037

INTRODUCTION

Investigation into the possibility of obtaining a superdense state of nuclear matter under laboratory conditions and into its properties is one of the most interesting problems in studying nuclear matter at various temperatures and densities [1]. At the same time, this is the main task in the physics programs for the future accelerator facilities NICA [2] and FAIR [3]. In heavy-ion collisions, however, a signal of the formation of superdense nuclear matter is accompanied by an enormous number of background particles. This renders such experiments quite involved methodologically and very complicated for a theoretical interpretation.

Yet another possibility is associated with the fact that a superdense state may be present in nuclear matter as a quantum component in the wave function. In processes involving high energy transfers and proceeding at short distances and times, one can visualize these quantum states. In interaction with a cold superdense component, characteristic signals must be observed not only in nucleus–nucleus but also in hadron-nucleus and lepton–nucleus collisions. An interaction with a dense configuration in nuclei must lead to an extension of the kinematical region beyond the limits admissible for free lepton–nucleon or hadron–nucleon interactions.

The idea that fluctuations of the nuclear density may exist in nuclei dates back to Blokhintsev's hypothesis [4]. Investigations of the kinematical region forbidden for processes involving free nucleons have been performed for many decades, and a large volume of experimental data has been obtained in these investigations (see, for example, [1, 5]). Processes leading to the production of particles in the kinematically forbidden region were called cumulative processes.

The region of high transverse momenta (P_T), where cumulative processes have not yet been studied experimentally, is of particular interest. A theoretical analysis performed in [6] revealed that, at $X_T \sim 1$, processes of interaction with multiquark (multinucleon) configurations must make a dominant contribution, the contribution of background rescattering processes being small. Here, X_T is a fraction of the maximum possible transverse momentum, $2P_T/\sqrt{s}$, with s being the invariant energy of nucleon–nucleon interaction.

The objective of the present study was to perform first measurements of inclusive spectra in the subcumulative and cumulative kinematical regions at high transverse momenta. The results obtained in the

[†]Deceased.
[1)]Institute for High Energy Physics, Protvino, Moscow oblast, 142284 Russia.
[2)]Joint Institute for Nuclear Research, Dubna, Moscow oblast, 141980 Russia.
[*]E-mail: Artem.Semak@ihep.ru

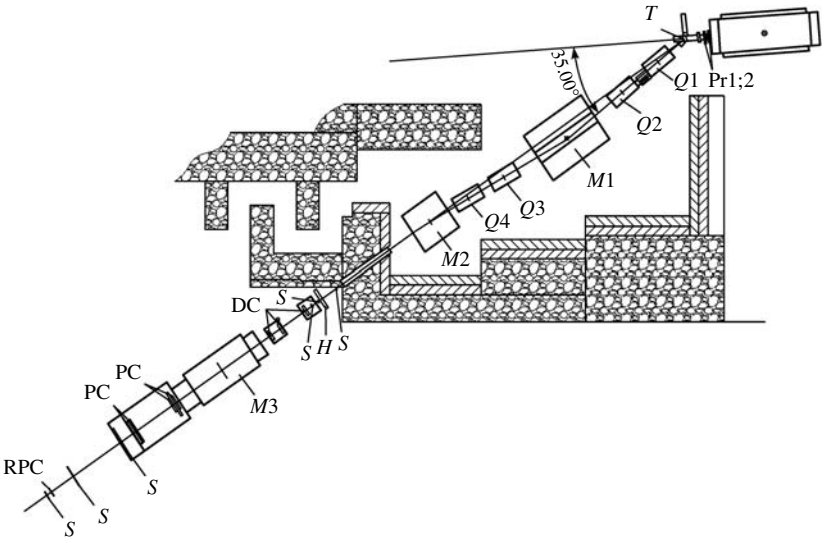

Fig. 1. Layout of the setup elements: (T) target, ($Q1$, $Q2$, $Q3$, and $Q4$) magnetic lenses, ($M1$ and $M2$) magnets pulling particles out of the hot zone, ($M3$) analyzing magnet, (S) set of scintillation trigger counters, (PC and DC) wire chambers of the tracker system, and (H and RPC) elements of the time-of-flight system (hodoscope and resistive planar chamber).

subcumulative region are compared with the predictions of existing popular Monte Carlo generators that are able to simulate proton–nucleus and nucleus–nucleus interactions.

1. SPIN SETUP AND DETAILS OF DATA ACQUISITION

In the present-day configuration, the SPIN setup is a narrow-aperture single-arm spectrometer. The layout of the setup is shown in Fig. 1. The equipment of the SPIN setup is deployed in two areas—a "hot" and a "cold" zone separated by a radiation shield. A beam profiler, a target, and six elements of setup's magnetic optics are situated in the hot zone. Measuring the position of six magnetic elements, one can select particles escaping from the target at angles in the range of 22°–55° and withdraw them through a channel in the shield to the cold zone housing the triggering and analyzing parts of the setup. In the present study, the data were accumulated for an angle of 35°. The coincidence of signals from five scintillation counters positioned upstream and downstream of an analyzing magnet ($M3$) serves as a trigger for a data-acquisition system. A system of wire chambers upstream of the magnet $M3$ and downstream of it makes it possible to measure the momentum of a particle with a resolution of $\sigma(p)/p \approx 3 \times 10^{-3}$. The angular acceptance of the setup is $\Delta\varphi \approx 100$ mrad in the azimuthal angle and $\Delta\theta \approx 40$ mrad in the polar angle. Its momentum acceptance changes from 5.5% at a momentum of 1 GeV/c to 3.5% at 6 GeV/c. The time-of-flight system consists of a scintillation hodoscope arranged at the inlet of the cold zone and a multigap planar chamber at the end of the spectrometer.

Table 1. Thicknesses of the targets used in the present study

Target	Carbon	Aluminum	Copper	Tungsten
Thickness [g/cm^2]	0.86	0.81	0.90	0.64

The data acquisition was performed in a proton beam extracted from the U-70 accelerator into beamline no. 8 at an intensity of about 5×10^{12} protons at the target per accelerator cycle. The spill duration was about 1 cm. Four thin targets were used; their thicknesses are given in Table 1.

All four targets were fixed on the same frame and were introduced in the beam alternately. Thus, the different targets were irradiated at close beam parameters. For each target, we measured the yield of charged particles having momenta in the range from 1.0 to 6.6 GeV/c; this corresponded to the transverse-momentum range of $P_T = 0.6$–3.7 GeV/c.

Background events are caused by particles that, without going along the spectrometer arm, penetrate into the cold zone and actuate trigger scintillation counters. In order to measure the contribution of background particles, a steel cylinder (shutter) four nuclear-length units long was installed at the very beginning of the spectrometer arm in between the first and second magnetic lenses ($Q1$ and $Q2$ in Fig. 1). The contribution of the background was measured in

Table 2. Values found for the parameters A, B, C, and D upon approximating measured spectra

Target nucleus	A, mb c GeV^{-1} sr^{-1}	B, c GeV^{-1}	C, c^2 GeV^{-2}	D, c^3 GeV^{-3}
C	629.8 ± 13.8	-1.626 ± 0.012	-0.272 ± 0.024	0.0146 ± 0.0005
Al	1165.0 ± 84.9	-1.473 ± 0.069	-0.266 ± 0.021	0.0132 ± 0.0019
Cu	3374.8 ± 190.9	-1.612 ± 0.056	-0.191 ± 0.016	0.0059 ± 0.0014
W	10290.0 ± 1116.8	-1.604 ± 0.102	-0.171 ± 0.029	0.0040 ± 0.0025

the case where the particle-propagation path along the spectrometer arm was locked by the shutter. By way of example, the fraction of background triggers as a function of the momentum of a positively charged particle is shown in Fig. 2 for two target nuclei used, carbon and tungsten. From this figure, one can see that the background contribution grows with momentum, amounting to about 13% at 6.6 GeV/c in the case of the carbon target. For tungsten, the background fraction at the maximum momentum is 4%. All of the experimental data presented below were corrected for the background contribution.

The proton-beam intensity was measured with the aid of a secondary-emission chamber. The transverse geometric parameters of the proton beam and its position were monitored with the aid of two-coordinate profilers equipped with sensitive electronics. The basic profiler parameters were the following: 16 channels per plane, the electrode step of 2.5 mm, and the thickness of 10 mg/cm^2.

2. DATA ON INCLUSIVE SPECTRA AND COMPARISON WITH PREDICTIONS OF THE UrQMD AND HIJING MODELS

For all four targets used, we constructed momentum spectra in the form of the double-differential cross section defined as

$$\frac{d^2\sigma}{dPd\Omega} = \frac{A}{N_A\rho t}\frac{1}{\varepsilon\Delta P\Delta\Omega}\frac{1}{N_{\text{ptot}}}N^{h^+},$$

where A is the number of intranuclear nucleons; N_A is the Avogadro number; ρ is the target density; t is the target thickness; Δp and $\Delta\Omega$ are, respectively, the momentum and solid-angle acceptances of the setup; N_{prot} is the total number of protons directed to the target; and N^{h^+} is the number of triggers for a given momentum. The quantity ε describes the losses arising upon the passage of particles over the long spectrometer arm (of length about 30 m) and the efficiency of the trigger system. The quantity $\varepsilon\Delta p\Delta\Omega$ was calculated via a simulation on the basis of the GEANT3 code, in which the parameters of all setup elements were embedded.

The double-differential cross sections measured for the production of positively charged particles versus the total momentum are presented in Fig. 3 for all four targets. The upper horizontal scale shows values of the transverse momentum P_T. The vertical dashed line corresponds to the kinematical limit for elastic proton–proton scattering. The region of transverse momenta in excess of about 2.5 GeV/c lies in the kinematical region forbidden for free-nucleon interaction. Thus, the data in Fig. 3 confirm the existence of cumulative particles in the region of high transverse momenta.

The statistical error in measured cross sections is less than 1% for momenta in the range of $P <$ 5 GeV/c. As the momentum grows above 5 GeV/c, this error increases and, at $P = 6.4$ GeV/c, amounts to 6% for tungsten and to 12% for carbon. The errors presented in Figs. 3–6 are purely statistical. The estimate of the systematic error in the measured cross sections was obtained by comparing data accumulated within different time periods. This error is momentum-independent and may be as large as about 20%. A dominant contribution to the systematic error comes from the uncertainty in mea-

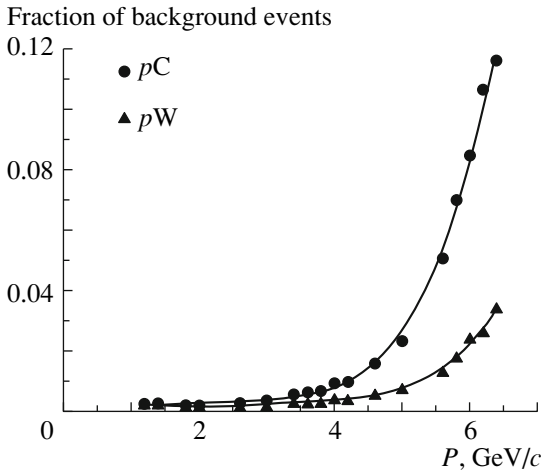

Fig. 2. Fraction of background events for various momentum values in the case of dealing with the carbon and tungsten targets.

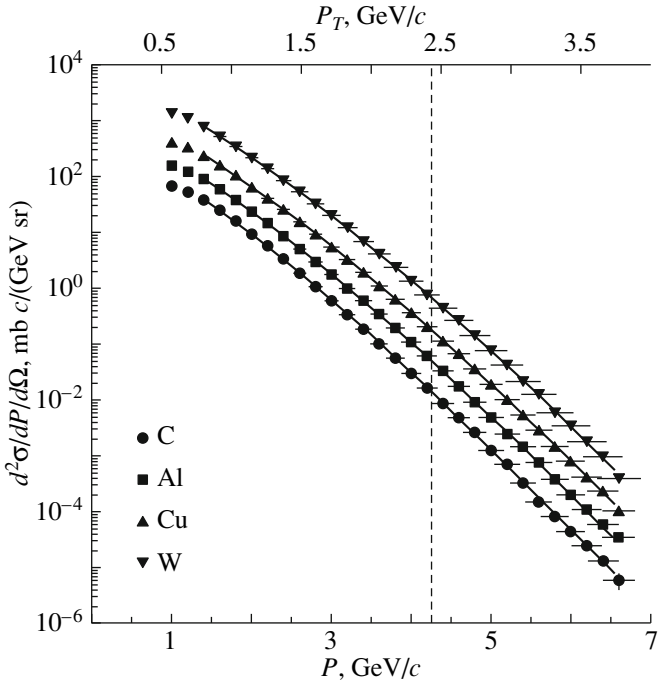

Fig. 3. Double-differential cross section for the production of positively charged particles emitted at an angle of 35° in proton interactions with four different targets. The vertical dashed line indicates the kinematical limit for elastic nucleon–nucleon (NN) scattering.

suring the number of beam particles that traversed the target. As was said above, the different targets were irradiated with a beam under close conditions. Therefore, a systematic error in measuring the cross-section ratio is smaller than that in measuring the cross sections themselves. The systematic error in measuring the cross-section ratio was estimated at about 7% by comparing the results of repeated measurements that were performed within different time periods.

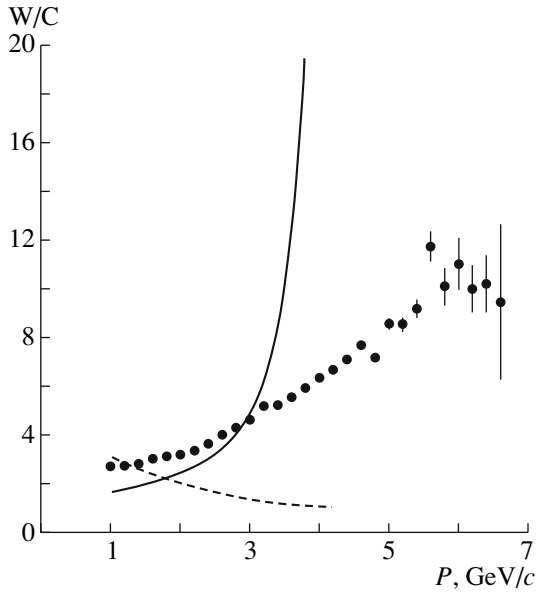

Fig. 4. Ratio of the yields of positively charged particles in proton interactions with tungsten and carbon targets: (points) experimental data, (dashed curve) predictions of the UrQMD model, and (solid curve) predictions of the HIJING model.

The solid curves in Fig. 3 represent the results obtained by approximating the differential spectra for momenta in the range of $P > 1.5$ GeV/c by the expression $A\exp(BP + CP^2 + DP^3)$, where A, B, C, and D are free parameters. The fitted values of A, B, C, and D and the errors in them are given in Table 2 for all target nuclei.

A comparison of the experimental data with the results of the calculations based on models that are applicable in the subcumulative region was performed for the ratio of the yields h^+ on the different targets. The experimental data were compared with the results of calculations performed within models popular in high-energy physics: UrQMD (version 3.3) [7] and HIJING (version 1.34) [8]. The UrQMD (Ultra-relativistic Quantum-Molecular-Dynamics model) code is a microscopic transport model in which one simulates multiparticle interactions of primary particles and newly produced particles, accomplishes the fragmentation of color strings into hadrons, and simulates the decay of hadronic resonances. This model

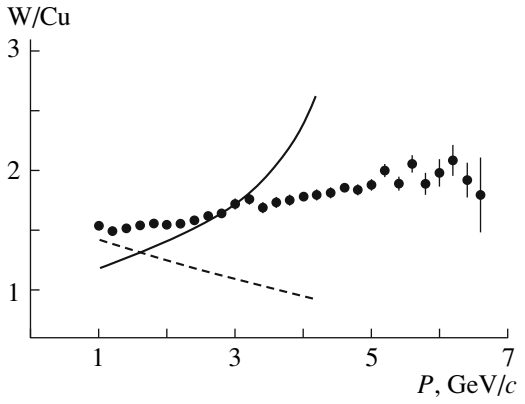

Fig. 5. As in Fig. 4, but for the case of the tungsten and copper targets.

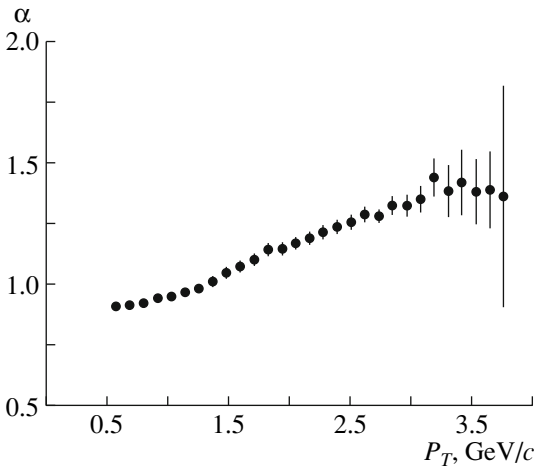

Fig. 6. Exponent in the power-law dependence of the cross section on the atomic number as a function of the transverse momentum.

is vigorously used to perform a comparison with data on hadron production in heavy-ion collisions. Examples of employing the UrQMD model can be found in the studies reported by the NA49 Collaboration in [9, 10]. The HIJING (Heavy Ion Jet INteraction Generator) code was created for describing particle production in proton–proton, proton–nucleus, and nucleus–nucleus interactions via a simulation of multiparticle jet production. A feature peculiar to HIJING is the inclusion of hard and semihard parton scattering accompanied by momentum transfers of several GeV units. Calculations performed on the basis of this model were used in [11, 12] to analyze data from experiments at the Relativistic Heavy Ion Collider (RHIC).

Figure 4 shows the measured ratios of the yields of particles on the tungsten and carbon targets per interaction event. Here, N_{int} is the number of interactions in the target. The experimental data in this figure are contrasted against the predictions of the (solid curve) HIJING and (dashed curve) UrQMD models. One can see that the predictions of HIJING and UrQMD do not comply with the measured values. A similar comparison of experimental data with the predictions of the same models is presented in Fig. 5, where the ratio of the yields on the tungsten and copper targets is shown. In just the same way as in the case of the W/C ratio, the experimental data for the W/Cu ratio are poorly described by the curves obtained upon the simulation.

Cumulative processes are characterized by a strong dependence on the atomic number [5]. In approximating the cross section by a power-law function that is proportional to A^α, the value of α for cumulative particles may be greater than unity. The exponent α obtained from the tungsten-to-carbon cross-section ratio is given in Fig. 6 as a function of the transverse momentum. This figure shows that α grows with P_T, reaching a value of about 1.37 at $P_T \approx 3.5$ GeV/c.

A strong A dependence may be due to the rescattering of secondary hadrons on intranuclear nucleons. In the present study, we did not attempt to estimate the contribution of this process. It should be noted, however, that, in [13–15], it was shown that, in reactions involving the production of antiprotons and other hadrons in proton–nucleus interactions at the proton energies of 10 and 70 GeV, the contribution of secondary interactions is small for particles of momentum in excess of 1 to 2 GeV/c.

CONCLUSIONS

Spectra of positively charged particles emitted at a laboratory angle of 35° in the interactions of 50-GeV protons with carbon, aluminum, copper, and tungsten nuclear targets have been obtained. The measurements have been performed in the transverse-momentum range extending up to $P_T = 3.7$ GeV/c and including the kinematically forbidden (cumulative) region of $P_T > 2.5$ GeV/c. The production of cumulative particles with high transverse momenta has been observed for the first time. The cross sections for the production of cumulative particles depends greatly on the target atomic number. The observation of high-P_T cumulative particles, together with a strong A dependence, may serve as an indication that our experiment has detected processes of hard scattering on dense multinucleon (multiquark) configurations in nuclei. It would be of interest to continue both experimental and theoretical investigations of the observed facts.

The spectra obtained in the subcumulative region deviate substantially from the respective predictions

of the standard Monte Carlo generators UrQMD and HIJING, which purport to describe proton–nucleus and nucleus–nucleus interactions.

ACKNOWLEDGMENTS

We are grateful to the directorate of the Institute for High Energy Physics for support of this investigation and to the personnel of the accelerator and beam departments for ensuring an efficient operation of the U-70 accelerator and beamline no. 8. Also, we are indebted to A.T. Golovin for his invaluable technical assistance in the preparation of the setup to performing measurements.

REFERENCES

1. G. A. Leksin, Phys. At. Nucl. **65**, 1985 (2002).
2. NICA Project, http://nica.jinr.ru
3. FAIR Project, http://www.fair-center.com
4. D. I. Blokhintsev, Sov. Phys. JETP **6**, 995 (1958).
5. A. V. Efremov, Sov. J. Part. Nucl. **13**, 254 (1982).
6. A. V. Efremov, V. T. Kim, and G. I. Lykasov, Sov. J. Nucl. Phys. **44**, 151 (1986).
7. S. A. Bass et al., Prog. Part. Nucl. Phys. **41**, 255 (1998); M. Bleicher et al., J. Phys. G **25**, 1859 (1999); http://urqmd.org
8. Xin-Nian Wang and M. Gyulassy, Phys. Rev. D **44**, 3501 (1991); http://www-nsdth.lbl.gov/~xnwang/hijing/doc.html
9. M. Mitrovski (for the NA49 Collab.), J. Phys. G **37**, 094003 (2010).
10. T. Anticic et al., Phys. Rev. C **79**, 044904 (2009).
11. J. T. Mitchel (for the PHENIX Collab.), J. Phys. Conf. Ser. **27**, 88 (2005).
12. A. Adare et al., Phys. Rev. C **78**, 044902 (2008).
13. L. M. Barkov et al., Sov. J. Nucl. Phys. **37**, 732 (1983); Sov. J. Nucl. Phys. **35**, 694 (1982).
14. A. A. Sibirtsev et al., Sov. J. Nucl. Phys. **53**, 121 (1991).
15. C. Pajares and Yu. M. Shabelski, *Relativistic Nuclear Interactions* (Editorial URSS, Moscow, 2007) [in Russian].

Translated by A. Isaakyan